BULLETIN OF THE POLISH ACADEMY OF SCIENCES
TECHNICAL SCIENCES, Vol. 59, No. 1, 2011
DOI: 10.2478/v10175-011-0014-1

Study of circular crested waves in a micropolar porous medium possessing cubic symmetry

R. KUMAR* and M. PANCHAL

Department of Mathematics, Kurukshetra University, Kurukshetra-136 119, India

Abstract. The paper is concerned with the propagation of circular crested Lamb waves in a homogeneous micpropolar porous medium possessing cubic symmetry. The frequency equations, connecting the phase velocity with wave number and other material parameters, for symmetric as well as antisymmetric modes of wave propagation are derived. The amplitudes of displacement components, microrotation and volume fraction field are computed numerically. The numerical results obtained have been illustrated graphically to understand the behavior of phase velocity and attenuation coefficient versus wave number of a wave.

Key words: cubic crystal, micropolar; porous; phase velocity; attenuation coefficient, frequency equation.

1. Introduction

The theory of elasticity concerning solid elastic material consisting of vacuous pores (voids) distributed throughout the body has become very important due to its theoretical and practical relevance. A non-linear theory in this respect has been formulated by Nunziato and Cowin [1]. Later Cowin and Nunziato [2] developed a theory of linear elastic materials with voids, for the mathematical study of the mechanical behavior of porous solids. They introduced the presence of pores in the classical continuum model by assigning an additional degree of freedom to each material particle, namely fraction of elementary volume which results void of matter; as a consequence, the bulk mass density of such materials is given by the product of two fields, the void volume fraction and the mass density of matrix material. The theory should well describe the mechanical behavior of porous geological materials, such as rocks and soils or porous manufactured materials such that ceramics and pressed powders, where the classical theory is inadequate.

Depending upon the mechanical properties, the materials of earth have been classified as elastic, viscoelastic, sandy, granular, microstructure etc. Some parts of earth may be supposed to be composed of material possessing micropolar/granular structure instead of continuous elastic materials.

To explain the fundamental departure of microcontinuum theories from the classical continuum theories, the former is a continuum model embedded with microstructures to describe the microscopic motion or a non local model to describe the long range material interaction. This extends the application of the continuum model to microscopic space and short-time scales. Micromorphic theory [3, 4] treats a material body as a continuous collection of a large number of deformable particles, with each particle possessing finite size and inner structure. Using assumptions such as infinitesimal deformation and slow motion, Micromorphic theory can be reduced to Mindlin's Microstructure theory [5]. When the microstructure of the material is considered rigid, it becomes the Micropolar theory [6].

Different researchers had discussed different type of problems in micropolar elasticity with voids. Scarpetta [7], Marin [8–11], discussed some problems in micropolar theory of elastic solids with voids. Passarella [12] derived the constitutive relations and field equations for anisotropic micropolar porous thermoelastic materials and also derived some basic results.

A cubic anisotropic medium possess three independent elastic constants compared to two for the isotropic media which are often assumed in classical elasticity. One result of constant is a coupling of terms in the Navier equations for a cubic medium. A wide class of crystals such as W, Si, Cu, Ni, Fe, Au and Al, which are frequently used substances, belong to the cubic materials. The cubic materials have nine planes of symmetry whose normals are on the three co-ordinate axes and on the co-ordinate planes making an angle of $\pi/4$ with the co-ordinate axes. With the chosen coordinate system along the crystalline directions, the mechanical behavior of a micropolar cubic crystal can be characterized by four independent elastic constants.

Cylindrical plates and panels are frequently used as structural components and their vibration characteristics are important for practical design. The waves which propagate in a freely vibrating plate are called Lamb waves. The unique properties of Lamb waves have made them increasingly attractive for nondestructive testing of bonded structures. The sensitivity and efficiency of adhesive bond inspection using Lamb waves has been the subject of study in recent years in many laboratories concerned with bond quality inspection. Kumar and Partap [13, 14] studied some problems concerning Rayleigh-Lamb waves and circular crested waves in micropolar isotropic elastic plate and microstretch elastic plate.

In the present paper we have discussed the propagation of circular crested waves in micropolar porous medium possessing cubic symmetry. Frequency equations relating the phase

*e-mail: rajneesh_kuk@rediffmail.com

velocity and wave number are derived for symmetric and anti-symmetric modes of wave propagation. The dispersion curves giving the phase velocity, attenuation coefficient as functions of wave number and amplitude ratios as functions of thickness of plate are plotted for anisotropic as well as for isotropic case.

2. Basic equations

Following Passarella [12], the constitutive relations and balance laws in general micropolar porous anisotropic medium possessing center of symmetry, in the absence of body forces, body couples, heat sources and extrinsic body force, are given by

Constitutive relations:

$$\begin{aligned} t_{ij} &= C_{ijkl}E_{kl} + G_{ijkl}\Psi_{kl} + H_{ij}\Phi, \\ m_{ij} &= G_{klji}E_{kl} + \Gamma_{jikl}\Psi_{kl} + P_{ji}\Phi, \\ g &= -H_{ij}E_{ij} - P_{ij}\Psi_{ij} - a\Phi - a_i\Phi_{,i}, \\ h_i &= a_i\Phi + D_{ij}\Phi_{,j}. \end{aligned} \tag{1}$$

The deformation and wryness tensor are defined by

$$E_{ji} = u_{i,j} + \epsilon_{ijk}\phi_k, \quad \Psi_{ij} = \phi_{i,j},$$

Balance laws:

$$\begin{aligned} t_{ij,j} &= \rho\ddot{u}_i, \\ m_{ij,j} - \epsilon_{irs}t_{rs} &= \rho\jmath\ddot{\phi}_i, \\ h_{i,i} + g &= \rho\chi\ddot{\Phi}, \end{aligned} \tag{2}$$

where t_{ij}, m_{ij} are respectively, the stress tensor and couple stress tensor, h_i is equilibrated stress vector, g is intrinsic equilibrated body force, ρ is bulk mass density, Φ is change in volume fraction, u_i, ϕ_i are respectively the components of displacement vector and microrotation vector.

C_{ijkl}, G_{ijkl}, Γ_{ijkl}, H_{ij}, D_{ij}, P_{ij}, a, a_i are characteristic constants of material following the symmetry properties given by Passarella [12].

3. Problem formulation and its solution

We have used appropriate transformations, following Atanackovic et al. [15], on the set of equations (1) to derive equations for micropolar porous cubic crystal. In the present case, we consider an infinite homogeneous plate of micropolar porous medium possessing cubic symmetry and of thickness $2d$. The plate is axi-symmetric with respect to z-axis as the axis of symmetry. We take the origin of the co-ordinate system (r, θ, z) on the middle surface of the plate and the z-axis is taken normal to the solid plate along the thickness. We take $r-z$ plane as the plane of incidence. If we restrict our analysis to the plane strain problem parallel to $r-z$ plane with the displacement vector $\overrightarrow{u} = (u_r, 0, u_z)$, microrotation vector $\overrightarrow{\phi} = (0, \phi_\theta, 0)$ and $\partial/\partial\theta = 0$, so that the field equations and constitutive relations in cylindrical polar coordinates reduce to

$$\frac{\partial t_{rr}}{\partial r} + \frac{\partial t_{zr}}{\partial z} + \frac{t_{rr} - t_{\theta\theta}}{r} = \rho\frac{\partial^2 u_r}{\partial t^2}, \tag{3}$$

$$\frac{\partial t_{rz}}{\partial r} + \frac{\partial t_{zz}}{\partial z} + \frac{t_{rz}}{r} = \rho\frac{\partial^2 u_z}{\partial t^2}, \tag{4}$$

$$\frac{\partial m_{r\theta}}{\partial r} + \frac{\partial m_{z\theta}}{\partial z} + \frac{m_{r\theta} + m_{\theta r}}{r} + t_{zr} - t_{rz} = \rho\jmath\frac{\partial^2\phi_\theta}{\partial t^2}, \tag{5}$$

$$\begin{aligned} D_1\left(\frac{\partial^2\Phi}{\partial r^2} + \frac{1}{r}\frac{\partial\Phi}{\partial r} + \frac{\partial^2\Phi}{\partial z^2}\right) - \\ -H_1\left(\frac{\partial u_r}{\partial r} + \frac{u_r}{r} + \frac{\partial u_z}{\partial z}\right) - a\Phi = \rho\chi\frac{\partial^2\Phi}{\partial t^2}, \end{aligned} \tag{6}$$

$$t_{rr} = C_{11}\frac{\partial u_r}{\partial r} + C_{12}\left(\frac{u_r}{r} + \frac{\partial u_z}{\partial z}\right) + H_1\Phi, \tag{7}$$

$$t_{rz} = C_{44}\left(\frac{\partial u_z}{\partial r} + \phi_\theta\right) + C_{45}\left(\frac{\partial u_r}{\partial z} - \phi_\theta\right), \tag{8}$$

$$t_{zr} = C_{44}\left(\frac{\partial u_r}{\partial z} - \phi_\theta\right) + C_{45}\left(\frac{\partial u_z}{\partial r} + \phi_\theta\right), \tag{9}$$

$$t_{\theta\theta} = C_{12}\left(\frac{\partial u_r}{\partial r} + \frac{\partial u_z}{\partial z}\right) + C_{11}\frac{u_r}{r} + H_1\Phi, \tag{10}$$

$$t_{zz} = C_{12}\left(\frac{\partial u_r}{\partial r} + \frac{u_r}{r}\right) + C_{11}\frac{\partial u_z}{\partial z} + H_1\Phi, \tag{11}$$

$$m_{r\theta} = \Gamma_{44}\frac{\partial\phi_\theta}{\partial r} - \Gamma_{45}\frac{\phi_\theta}{r}, \tag{12}$$

$$m_{\theta r} = \Gamma_{45}\frac{\partial\phi_\theta}{\partial r} - \Gamma_{44}\frac{\phi_\theta}{r}, \tag{13}$$

$$m_{z\theta} = \Gamma_{44}\frac{\partial\phi_\theta}{\partial z}. \tag{14}$$

Let us now introduce the dimensionless quantities as

$$\begin{aligned} r' &= \frac{\omega^*}{c_1}r, \qquad z' = \frac{\omega^*}{c_1}z, \qquad u_r' = \frac{\omega^*}{c_1}u_r, \\ u_z' &= \frac{\omega^*}{c_1}u_z, \qquad \phi_\theta' = \frac{C_{11}}{C_{45}}\phi_\theta, \qquad \Phi' = \frac{C_{11}}{C_{45}}\Phi, \\ t_{zz}' &= \frac{t_{zz}}{C_{11}}, \qquad t_{zr}' = \frac{t_{zr}}{C_{11}}, \qquad m_{z\theta}' = \frac{c_1}{\Gamma_{44}\omega^*}m_{z\theta}, \\ t' &= \omega^* t, \qquad c_1^2 = \frac{C_{11}}{\rho}, \qquad \omega^{*2} = \frac{C_{45}}{\rho\jmath}. \end{aligned} \tag{15}$$

Using dimensionless variables defined by (15) in Eqs. (3)–(6) with the help of (7)–(14), after suppressing the primes the field equations reduce to

$$\begin{aligned} \left(\frac{\partial^2 u_r}{\partial r^2} + \frac{1}{r}\frac{\partial u_r}{\partial r} - \frac{u_r}{r^2}\right) + a_1\frac{\partial^2 u_r}{\partial z^2} + a_2\frac{\partial^2 u_z}{\partial r\partial z} + \\ +a_3\frac{\partial\phi_\theta}{\partial z} + a_4\frac{\partial\Phi}{\partial r} = \frac{\partial^2 u_r}{\partial t^2}, \end{aligned} \tag{16}$$

$$\begin{aligned} a_1\left(\frac{\partial^2 u_z}{\partial r^2} + \frac{1}{r}\frac{\partial u_z}{\partial r}\right) + \frac{\partial^2 u_z}{\partial z^2} + \\ +a_2\left(\frac{\partial^2 u_r}{\partial r\partial z} + \frac{1}{r}\frac{\partial u_r}{\partial z}\right) - a_3\left(\frac{\partial\phi_\theta}{\partial r} + \frac{\phi_\theta}{r}\right) + \\ +a_4\frac{\partial\Phi}{\partial z} = \frac{\partial^2 u_z}{\partial t^2}, \end{aligned} \tag{17}$$

$$\begin{aligned} \frac{\partial^2\phi_\theta}{\partial r^2} + \frac{\partial^2\phi_\theta}{\partial z^2} + \frac{1}{r}\frac{\partial\phi_\theta}{\partial r} - \frac{\phi_\theta}{r^2} + \\ +a_5\left(\frac{\partial u_z}{\partial r} - \frac{\partial u_r}{\partial z}\right) + 2a_6\phi_\theta = a_7\frac{\partial^2\phi_\theta}{\partial t^2}, \end{aligned} \tag{18}$$

$$\nabla^2\Phi - a_8\left(\frac{\partial u_r}{\partial r} + \frac{u_r}{r} + \frac{\partial u_z}{\partial z}\right) - a_9\Phi = a_{10}\frac{\partial^2\Phi}{\partial t^2}, \quad (19)$$

where

$$\begin{gathered}
\nabla^2 = \frac{\partial^2}{\partial r^2} + \frac{1}{r}\frac{\partial}{\partial r} + \frac{\partial^2}{\partial z^2}, \\
a_1 = \frac{C_{44}}{C_{11}}, \qquad a_2 = \frac{C_{12}+C_{45}}{C_{11}}, \\
a_3 = \frac{(C_{45}-C_{44})C_{45}}{C_{11}^2}, \qquad a_4 = \frac{H_1 C_{45}}{C_{11}^2}, \\
a_5 = \frac{(C_{45}-C_{44})C_{11}c_1^2}{\Gamma_{44}C_{45}\omega^{*2}}, \\
a_6 = \frac{(C_{45}-C_{44})c_1^2}{\Gamma_{44}\omega^{*2}}, \\
a_7 = \frac{\rho\jmath c_1^2}{\Gamma_{44}}, \qquad a_8 = \frac{H_1 C_{11}c_1^2}{D_1 C_{45}\omega^{*2}}, \\
a_9 = \frac{ac_1^2}{D_1\omega^{*2}}, \qquad a_{10} = \frac{\rho\chi c_1^2}{D_1}.
\end{gathered} \quad (20)$$

Assuming the solutions of Eqs. (16)–(19) for the waves propagating in the z-direction as

$$\begin{gathered}
\{u_r, u_z, \phi_\theta, \Phi\} = \\
= \{J_1(\xi r), \overline{u}_z J_0(\xi r), \overline{\phi}_\theta J_1(\xi r), \overline{\Phi} J_0(\xi r)\} u_r e^{\imath\xi(mz-ct)},
\end{gathered} \quad (21)$$

where $\omega(=\xi c)$ is the angular frequency, ξ is the wave number and c is the phase velocity. m is an unknown parameter which signifies the penetration depth of the wave; $\overline{u}_z$, $\overline{\phi}_\theta$, $\overline{\Phi}$ are respectively the amplitude ratios of the displacement component u_z, microrotation ϕ_θ, and volume fraction field Φ to that of the displacement component u_r. $J_0()$ and $J_1()$ are the Bessel functions of order zero and one respectively.

Substituting (21) in Eqs. (16)–(19), we obtain

$$\begin{gathered}
\xi^2(c^2 - 1 - a_1 m^2) + \imath\xi^2 m a_2 \overline{u}_z + \\
+\imath\xi m a_3 \overline{\phi}_\theta - \xi a_4 \overline{\Phi} = 0, \\
\imath\xi^2 m a_2 + \xi^2(c^2 - a_1 - m^2)\overline{u}_z - \\
-\xi a_3 \overline{\phi}_\theta + \imath\xi m a_4 \overline{\Phi} = 0, \\
-\imath\xi m a_5 - \xi a_5 \overline{u}_z + \\
+\{\xi^2(a_7 c^2 - 1 - m^2) + 2a_6\}\overline{\phi}_\theta + 0.\overline{\Phi} = 0, \\
-\xi a_8 - \imath\xi m a_8 \overline{u}_z + 0.\overline{\phi}_\theta + \\
+\{\xi^2(a_{10}c^2 - 1 - m^2) - a_9\}\overline{\Phi} = 0.
\end{gathered} \quad (22)$$

For the non-trivial solution of the system of Eqs. (22), the determinant of coefficients of $1, \overline{u}_z, \overline{\phi}_\theta$ and $\overline{\Phi}$ must vanish which gives

$$m^8 + Am^6 + Bm^4 + Cm^2 + D = 0, \quad (23)$$

where

$$A = \frac{1}{\xi^2 a_1}\{a_2^2 - a_1 b_1 - a_3 a_5 - b_2\},$$

$$B = \frac{1}{\xi^4 a_1}\{\xi^2(a_2 b_7 + (a_2 - 1)a_4 a_8) + a_1 b_5 + a_3 b_9 + b_2 b_4\},$$

$$C = \frac{1}{\xi^6 a_1}\{\xi^2(a_2 b_8 + a_4 a_8 b_{11}) - a_1 b_6 - a_3 b_{10} - b_2 b_5\},$$

$$D = \frac{1}{\xi^8 a_1}\{a_4 b_{12}\xi + b_2 b_6\},$$

$$b_1 = \xi^2(c^2 - a_1),$$

$$b_2 = \xi^2(a_7 c^2 - 1) + 2a_6,$$

$$b_3 = \xi^2(a_{10}c^2 - 1) - a_9,$$

$$b_4 = a_4 a_8 + b_1 + b_2 + b_3,$$

$$b_5 = b_1 b_2 + b_2 b_3 + b_3 b_1 + a_4 a_8 b_2 - a_3 a_5 \xi^2,$$

$$b_6 = (b_1 b_2 - a_3 a_5 \xi^2) b_3,$$

$$b_7 = a_3 a_5 - a_4 a_8 - a_2(b_2 + b_3),$$

$$b_8 = (a_2 b_2 - a_3 a_5 + a_4 a_8) b_3,$$

$$b_9 = (b_1 + b_3 - a_2 + a_4 a_8) a_5,$$

$$b_{10} = (b_1 b_3 - \xi^2(a_2 b_3 + a_4 a_8)) a_5,$$

$$b_{11} = (b_1 + b_2 - a_2 b_2 + a_3 a_5),$$

$$b_{12} = \xi a_8(a_3 a_5 \xi^2 - b_1 b_2).$$

The roots of Eq. (23) are complex in general. These roots are denoted by m_j^2, $j = 1, \ldots, 4$. Thus the appropriate solutions of (16)–(19), corresponding to the wave propagating along z-axis are

$$\begin{gathered}
\{u_r, u_z, \phi_\theta, \Phi\} = \sum_{j=1}^{4}(E_j cos\xi m_j z + F_j sin\xi m_j z)\cdot \\
\cdot\{J_1(\xi r), r_j J_0(\xi r), l_j J_1(\xi r), t_j J_0(\xi r)\} e^{-\imath\omega t},
\end{gathered} \quad (24)$$

where

$$r_j = -\frac{\Delta_2(j)}{\Delta_1(j)},$$

$$l_j = \frac{\Delta_3(j)}{\Delta_1(j)},$$

$$t_j = -\frac{\Delta_4(j)}{\Delta_1(j)},$$

$$\Delta_1(j) = -\xi^6 m_j^6 + b_4\xi^4 m_j^4 - b_5\xi^2 m_j^2 + b_6,$$

$$\Delta_2(j) = \imath\xi^2 m_j\{a_2\xi^2 m_j^4 + b_7\xi^2 m_j^2 + b_8\}$$

$$\Delta_3(j) = \imath\xi m_j\{a_5\xi^4 m_j^4 - b_9\xi^2 m_j^2 + b_{10}\},$$

$$\Delta_4(j) = (a_2 - 1)a_8\xi^5 m_j^4 + b_{11}\xi^3 m_j^2 + b_{12}.$$

3.1. Derivation of frequency equation. At the surfaces $z = \pm d$, the appropriate boundary conditions are

$$\begin{aligned} t_{zz} &= 0, \qquad t_{zr} = 0, \\ m_{z\theta} &= 0, \qquad \frac{\partial \Phi}{\partial z} = 0, \end{aligned} \tag{25}$$

where t_{zz}, t_{zr} are the normal and tangential stress components, $m_{z\theta}$ is the tangential couple stress. Making use of (24) in Eqs. (9), (11) and (14) and then using boundary conditions (25), we obtain eight homogeneous equations in eight unknowns $E_1, \ldots, E_4, F_1, \ldots, F_4$. The condition for the non-trivial solution of these equations yields the frequency equation

$$\begin{aligned} &[T_1T_2]^{\pm 1}AT1 + [T_1T_3]^{\pm 1}AT2 + \\ &+ [T_1T_4]^{\pm 1}AT3 + [T_2T_3]^{\pm 1}AT4 + \\ &+ [T_2T_4]^{\pm 1}AT5 + [T_3T_4]^{\pm 1}AT6 = 0, \end{aligned} \tag{26}$$

where power '$+1$' corresponds to the skew-symmetric mode and '-1' corresponds to the symmetric mode of wave propagation,

$$\begin{aligned} T_i &= \tan(m_i \xi H) \qquad i = 1, \ldots, 4, \\ AT1 &= m_3 m_4 (l_3 t_4 - l_4 t_3)(G_{11}G_{22} - G_{12}G_{21}), \\ AT2 &= m_2 m_4 (l_2 t_4 - l_4 t_2)(G_{13}G_{21} - G_{11}G_{23}), \\ AT3 &= m_2 m_3 (l_2 t_3 - l_3 t_2)(G_{11}G_{24} - G_{14}G_{21}), \\ AT4 &= m_1 m_4 (l_1 t_4 - l_4 t_1)(G_{12}G_{23} - G_{13}G_{22}), \\ AT5 &= m_1 m_3 (l_1 t_3 - l_3 t_1)(G_{14}G_{22} - G_{12}G_{24}), \\ AT6 &= m_1 m_2 (l_1 t_2 - l_2 t_1)(G_{13}G_{24} - G_{14}G_{23}), \end{aligned}$$

$$\begin{aligned} G_{1j} &= a_{11}\xi + a_4 t_j, \\ G_{2j} &= a_{12}\xi r_j - a_3 l_j, \qquad j = 1, \ldots, 4, \\ a_{11} &= \frac{C_{12}}{C_{11}}, \\ a_{12} &= \frac{C_{45}}{C_{11}}. \end{aligned}$$

Equation (26) determines the dimensionless phase velocity c of axi-symmetric surface waves as a function of dimensionless wave number ξ and other micropolar parameters of the medium.

4. Amplitudes of displacements and microrotation and volume fraction field

The amplitudes of displacement components, microrotation and volume fraction field for symmetric and antisymmetric modes of plane waves can be obtained as:

$$\begin{aligned} &((u_r)_{sy}, (u_r)_{asy}) = \\ &= \sum_{j=1}^{4} (E_j \cos(\xi m_j y), F_j \sin(\xi m_j y)) J_1(\xi r) e^{-\imath\omega t}, \\ &((u_z)_{sy}, (u_z)_{asy}) = \\ &= \sum_{j=1}^{4} r_j (F_j \sin(\xi m_j y), E_j \cos(\xi m_j y)) J_0(\xi r) e^{-\imath\omega t}, \\ &((\phi_\theta)_{sy}, (\phi_\theta)_{asy}) = \\ &= \sum_{j=1}^{4} l_j (F_j \sin(\xi m_j y), E_j \cos(\xi m_j y)) J_1(\xi r) e^{-\imath\omega t}, \\ &(\Phi_{sy}, \Phi_{asy}) = \\ &= \sum_{j=1}^{4} t_j (E_j \cos(\xi m_j y), F_j \sin(\xi m_j y)) J_0(\xi r) e^{-\imath\omega t}. \end{aligned} \tag{27}$$

5. Particular case

I) Neglecting the porous effect i.e. vanishing H_1, D_1, a and χ, we obtain the corresponding expressions for micropolar cubic crystal.

II) Taking $C_{11} = \lambda + 2\mu + K$, $C_{12} = \lambda$, $C_{44} = \mu + K$, $C_{45} = \mu$, $\Gamma_{44} = \gamma$, $D_1 = \alpha^*$, $H_1 = \beta^*$ and $a = \varsigma^*$, we obtain the corresponding expressions for the micropolar porous isotropic medium with the changed values of $m_i (i = 1, \ldots, 4)$.

6. Numerical results and discussion

For numerical computation, we take the following values of relevant parameters for micropolar porous cubic crystal as

$$\begin{aligned} C_{11} &= 26 \times 10^{10} \text{ N/m}^2, \\ C_{12} &= 20 \times 10^{10} \text{ N/m}^2, \\ C_{44} &= 6.5 \times 10^{10} \text{ N/m}^2, \\ C_{45} &= 5.3 \times 10^{10} \text{ N/m}^2, \\ \Gamma_{44} &= .98 \times 10^{-9} \text{ N}, \\ H_1 &= 2.41 \times 10^{10} \text{ N/m}^2, \\ D_1 &= 2.3 \times 10^{-9} \text{ N}, \\ a &= 2.181 \times 10^{10} \text{ N/m}^2. \end{aligned}$$

For comparison with micropolar porous isotropic solid, following Eringen [16], we take the following values of relevant parameters of micropolar isotropic solid for the case of Magnesium crystal like material as

$$\rho = 1.74 \times 10^3 \text{ Kg/m}^3,$$

$$\lambda = 9.4 \times 10^{10} \text{ N/m}^2,$$

$$\mu = 4.0 \times 10^{10} \text{ N/m}^2,$$

$$K = 1.0 \times 10^{10} \text{ N/m}^2,$$

$$\gamma = 0.779 \times 10^{-9} \text{ N},$$

$$\jmath = 0.2 \times 10^{-19} \text{ m}^2,$$

The void parameters are,

$$\alpha^* = 1.44 \times 10^{-9} \text{ N},$$

$$\beta^* = 1.328 \times 10^{10} \text{ N/m}^2,$$

$$\varsigma^* = 1.103 \times 10^{10} \text{ N/m}^2,$$

$$\chi = .995 \times 10^{-19} \text{ m}^2.$$

and the dimensionless thickness of the plate is taken as $d = 0.07$.

Equation (26) determine the phase velocity c of the surface waves as a function of wave number ξ and various physical parameters in complex form. If we write

$$\frac{1}{c} = \frac{1}{v} + \imath\frac{q}{\omega}, \tag{28}$$

then wave number $\xi = R + \imath q$, where R=ω/v and q are real numbers. This shows that v is propagation speed and q is attenuation coefficient of the surface waves. The graphical representation is given to depict the behavior of phase velocity (Fig. 1 for symmetric and Fig. 2 for antisymmetric modes) and attenuation coefficient (Fig. 3 for symmetric and Fig. 4 for antisymmetric modes) with respect to R i.e. real part of wave number, Figs. 5–8 represent, respectively, the variation of amplitudes of tangential component of displacement, normal component of displacement, microrotation and volume fraction field with respect to thickness of plate, to compare the results for micropolar porous isotropic solid (MPIS) and micropolar porous cubic crystal (MPCC). In Figs. 1–4, the solid lines, small dashed lines and long dashed lines represent respectively the first ($n = 1$), second ($n = 2$) and third ($n = 3$) in case of MPCC whereas the corresponding lines with central symbol diamond represent the same situation in case of MPIS. In Figs. 5–8 the solid lines and dashed lines represent, respectively, the variation of amplitudes for antisymmetric and symmetric mode in case of MPCC whereas the corresponding lines with central symbol represent the same situation in case of MPIS.

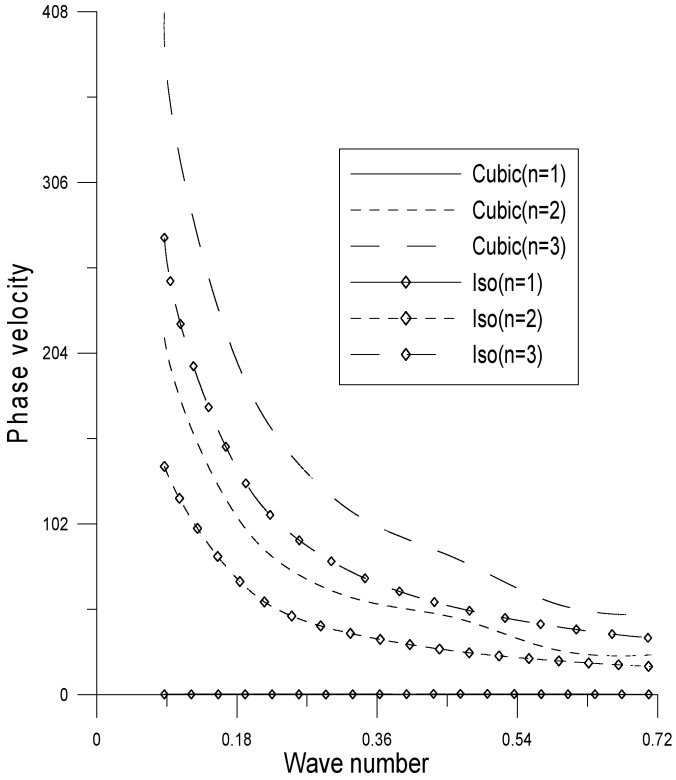

Fig. 1. Variation of phase velocity w.r.t wave number for symmetric modes of wave propagation

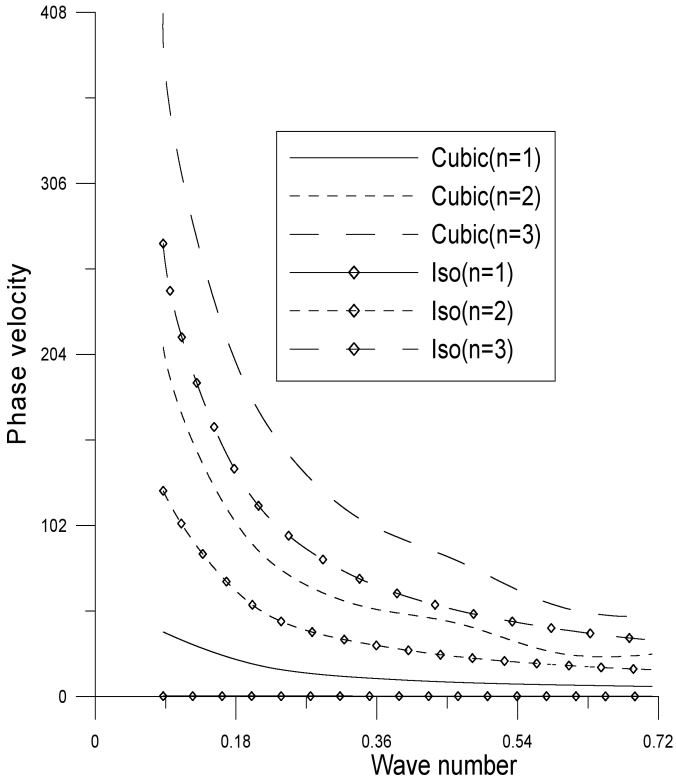

Fig. 2. Variation of phase velocity w.r.t wave number for antisymmetric modes of wave propagation

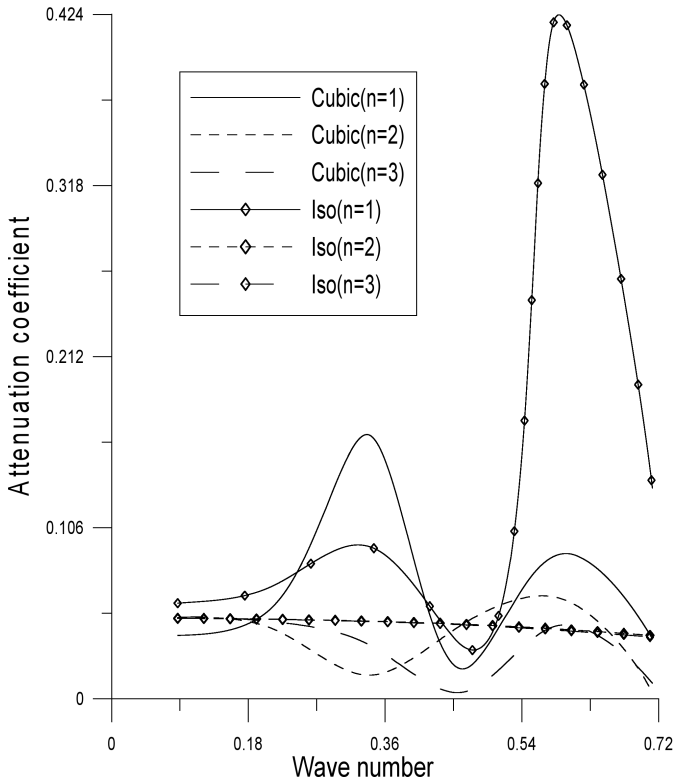

Fig. 3. Variation of attenuation coefficient w.r.t wave number for symmetric modes of wave propagation

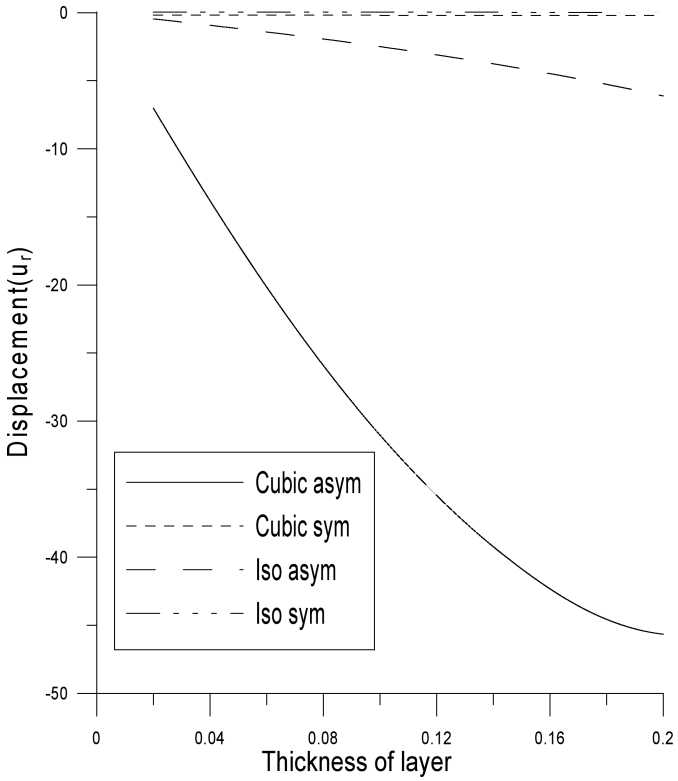

Fig. 5. Variation of amplitude of displacement component (u_r) w.r.t thickness of layer

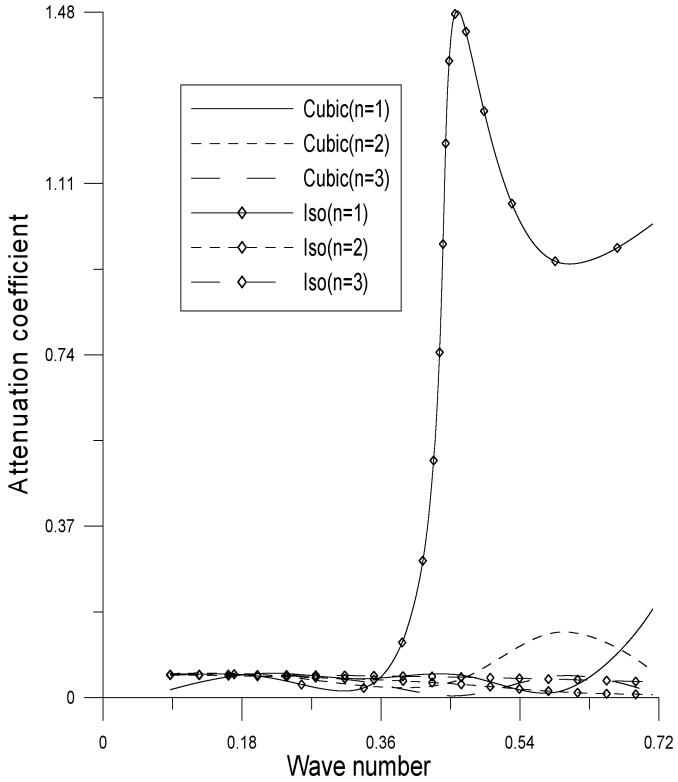

Fig. 4. Variation of attenuation coefficient w.r.t wave number for anti-symmetric modes of wave propagation

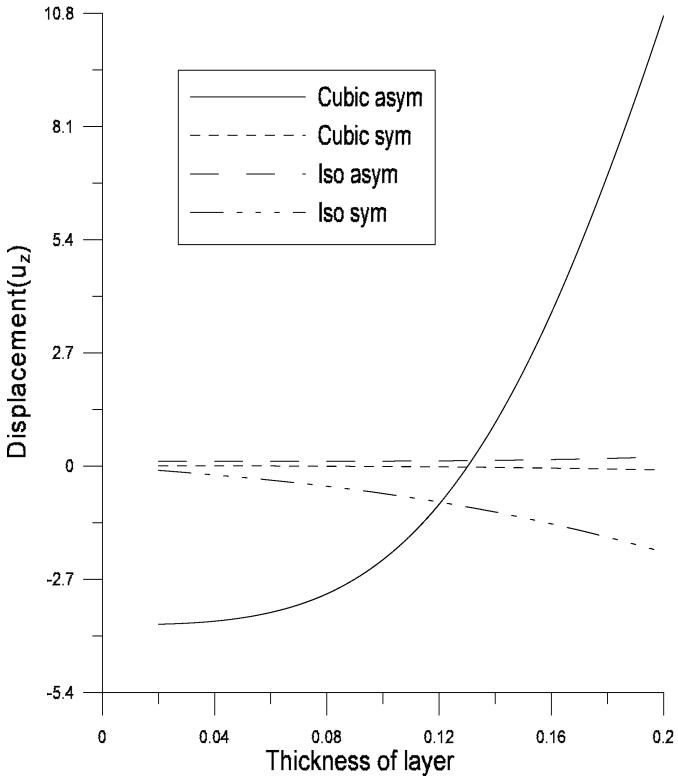

Fig. 6. Variation of amplitude of displacement component (u_z) w.r.t thickness of layer

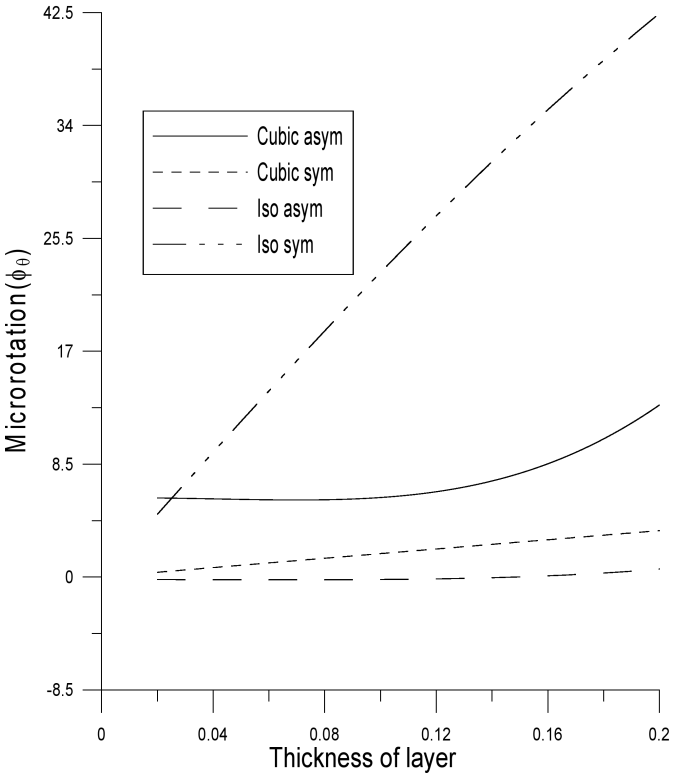

Fig. 7. Variation of amplitude of microrotation(ϕ_θ) w.r.t thickness of layer

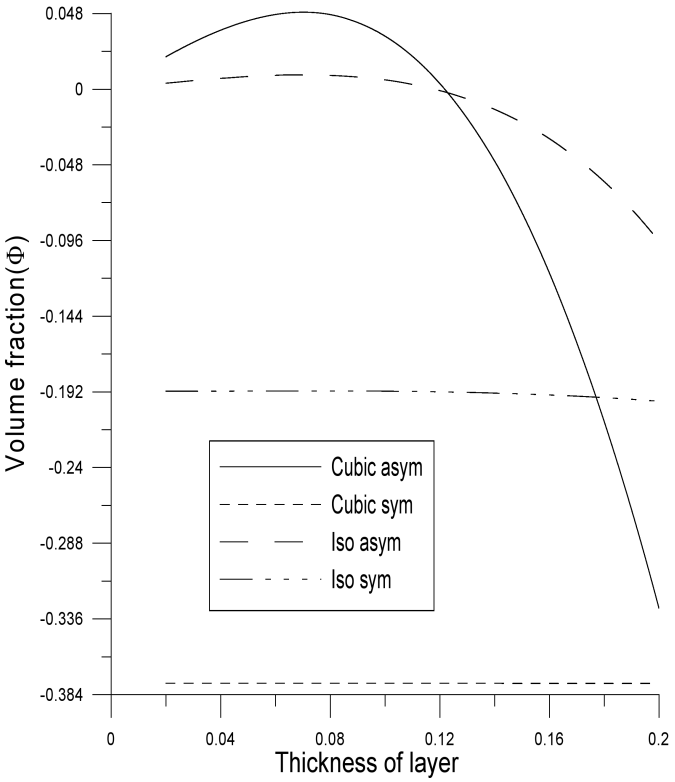

Fig. 8. Variation of amplitude of volume fraction (Φ) w.r.t thickness of layer

Phase velocity. It is observed from Figs. 1 and 2 that the behavior and trend of variation of phase velocity for symmetric modes is same as that for antisymmetrc modes of wave propagation except for the difference in magnitude values. The phase velocity of different modes of wave propagation start from large values at vanishing wave number and then exhibits a strong dispersion until the velocity flattens out to the value of Rayleigh wave velocity at higher wave number. The reason for the asymptotic approach is that for short wavelengths(or high frequencies), the material plate behaves increasingly like a thick slab and hence the coupling between the upper and lower boundary surfaces is reduced and as a result the properties of symmetric and antisymmetric modes of wave propagation become more and more similar. In the limit for an infinite thick slab, the motion at the upper surface is not confined to the lower surface and the displacements become localized near the free boundaries, thus the Lamb wave dispersion curves asymptotically approach those for Rayleigh waves. The value of phase velocity is higher for the higher number of mode of wave propagation within the whole range and for a particular mode of wave propagation, the value of phase velocity is higher for MPCC as compared to that for MPIS.

Attenuation coefficient. The variation of attenuation coefficient with respect to wave number is depicted in Figs. 3 and 4 for symmetric and antisymmetric modes respectively. It is observed that the attenuation coefficient shows an oscillating behavior for all the modes of wave propagation. The peak value of attenuation coefficient is highest in case of MPIS for the lowest mode ($n = 1$) of wave propagation in both symmetric as well as antisymmetric cases. For symmetric modes ($n = 2, 3$), the values of attenuation coefficient in case of MPIS appears to be constant as compared to those in case of MPCC. In case of MPCC and for lowest symmetric mode ($n = 1$), the values of attenuation coefficient oscillate within the range $0.09 < R < .63$ and increase beyond this range. In case of MPCC, antisymmetric modes ($n = 2, 3$), the values of attenuation coefficient are of oscillating behavior within the whole range with amplitude of oscillation higher for ($n = 2$) as compared to that for ($n = 3$). In case of MPIS and antisymmetric modes ($n = 2, 3$), the values of attenuation coefficient decrease linearly with respect to wave number within the whole range.

Amplitudes. The variation of amplitudes of displacement components, microrotation and volume fraction field is depicted in Figs. 5–8 respectively. It is observed from Fig. 5 that the values of amplitudes of displacement component (u_r) for antisymmetric mode of wave propagation decreases in case of both MPIS and MPCC whereas the values for symmetric mode remain almost constant as compared to those for antisymmetric modes. Also the values for symmetric mode are higher as compared to those for antisymmetric mode for both MPIC and MPCC and for a particular mode of wave propagation, the values in case MPIS are higher than those in case of MPCC. Figure 6 indicates that the values of amplitude of displacement component (u_z) for antisymmetric modes increase in case of MPCC and remain almost constant in case of MPIS whereas for symmetric mode, the values remain consant

for MPCC and decrease for MPIS. For symmetric mode, the values for MPCC are higher than those for MPIS whereas for antisymmetric mode, the values for MPIS are higher than those for MPCC within the range $0-0.12$, but the behavior is reversed after this range. Figure 7 indicates that the values of amplitude of microrotation (ϕ_θ) increase with the thickness of layer in all cases. The values for antisymmetric mode are higher in case of MPCC as compared to those in case of MPIS whereas the behavior is reverse for symmetric mode. In case of MPCC, the values for antisymmetric mode are higher than those for symmetric mode whereas the behavior is reversed in case of MPIS. It is observed from Fig. 8 that the values of amplitude of volume fraction field (Φ) for antisymmetric mode first increase slightly and then decrease continuously within the whole range whereas for symmetric mode of wave propagation, the values remain constant for both MPIS and MPCC.

7. Conclusions

The propagation of circular crested waves in homogeneous layer of micropolar porous cubic crystal like material is investigated after deriving secular equations. The phase velocity of higher modes of wave propagation for symmetric and antisymmetric modes attain quite large values at vanishing wave number which sharply flattens out to become steady and asymptotic to the Rayleigh wave velocity with increasing wave number. The reason is that in the limit of an infinite thick slab the motion at the upper surface is not confined to the lower surface and the displacements become localized near the free boundaries, thus the Lamb wave dispersion curves asymptotically approach to those for Rayleigh waves. The behavior of attenuation coefficient is oscillating for almost all the curves for both symmetric and antisymmetric modes. An appreciable effect of anisotropy is observed on the phase velocity, attenuation coefficient and amplitude ratios for all the components.

REFERENCES

[1] J.W. Nunziato and S.C. Cowin, "A non-linear theory of elastic materials with voids", *Arch. Rat. Mech. Anal*. 72, 175–201 (1979).

[2] S.C. Cowin and J.W. Nunziato, "Linear elastic materials with voids", *J. Elasticity* 13, 125–147 (1983).

[3] E.S. Suhubi and A.C. Eringen, "Non-linear theory of simple microelastic solids II", *Int. J. Engng. Sci.* 2, 389–404 (1964).

[4] A.C. Eringen, *Microcontinuum Field Theories I: Foundations and Solids*, Springer-Verlag, New York, 1999.

[5] R.D. Mindlin, "Microstructure in linear elasticity", *Arch. Rational Mech. Anal.* 16, 51–78 (1964).

[6] A.C. Eringen, "Linear theory of micropolar elasticity", *J. Math. Mech.* 16, 909–923 (1966).

[7] E. Scarpetta, "On the fundamental solutions in micropolar elasticity with voids", *Acta. Mechanica* 82, 151–158 (1990).

[8] M. Marin, "The mixed problem in elastostatic of micropolar materials with voids", *An: Stiinf Uni. Ovidivs Constanta Ser. Mat.* 3, 106–117 (1995).

[9] M. Marin, "Some basic theorems in elastostatics of micropolar materials with voids", *J. Comput. Appl. Math.* 70, 115–126 (1996).

[10] M. Marin, "Generalized solutions in elasticity of micropolar bodies with voids", *Rev. Acad. Canaria. Cienc.* 8, 101–106 (1996).

[11] M. Marin, "A temporally evolutionary equation in elasticity of micropolar bodies with voids", *Bull. Ser. Appl. Math. Phys.* 60, 3–12 (1998).

[12] F. Passarella, "Some results in micropolar thermoelasticity", *Mechanics Research Communications* 23, 349–357 (1996).

[13] R. Kumar and G. Partap, "Rayleigh Lamb waves in a micropolar isotropic elastic plate", *Applied Mathematics and Mechnics* 27, 1049–1059 (2006).

[14] R. Kumar and G. Partap, "Circular crested waves in a microstretch elastic plate", *Science and Engineering of Composite Materials* 14, 251–269 (2007).

[15] T.M. Atanackovic and A. Guran, *Theory of Elasticity for Scientists and Engineers*, Birkhauser, Klosterberg, 2000.

[16] A.C. Eringen, "Plane waves in nonlocal micropolar elasticity", *Int. J. Engng. Sci.* 22, 1113–1121 (1984).